Supporting Information

Molecular Structure of RADA16-I Designer Self-Assembling Peptide Nanofibers

Ashley R. Cormier[1,2], Xiaodong Pang[3], Maxwell I. Zimmerman[1,2], Huan-Xiang Zhou[3], Anant K. Paravastu[1, 2]*

[1]Department of Chemical and Biomedical Engineering, FAMU-FSU College of Engineering, 2525 Pottsdamer Street, Tallahassee, FL 32310-6046
[2]National High Magnetic Field Laboratory, 1800 E. Paul Dirac Drive, Tallahassee, FL 32310
[3]Department of Physics and Institute of Molecular Biophysics, Florida State University, Tallahassee, FL 32306

*Address correspondence to paravastu@eng.fsu.edu

Supporting Information

Cormier *et al*.

SI Text

Supplementary Methods:

Peptide Preparation

RADA16-I was synthesized on an Applied Biosystems Model 433A Peptide Synthesizer without labels for the natural abundance sample as well as with various isotopic labels incorporated using labeled FMOC-protected amino acids purchased from Cambridge Isotopes or Sigma-Aldrich (see Table 1). An FMOC rink-amide resin (Anaspec, Inc.; 0.45 meq/g) was used for synthesis. The synthesized peptides were cleaved from the resin using standard procedures and were then dissolved in formic acid (5% in water) as described previously.[1] The samples were then frozen in liquid nitrogen and lyophilized on a Virtis Benchtop K freeze dryer. The peptides were purified using HPLC on a Beckman Coulter System Gold 125 Solvent Module with a System Gold 166 Detector and a Waters C18-bonded silica semi-preparative column. Mass spectrometry was performed for peptide verification on a Jeol Accutof JMS-T100LC Mass Spectrometer with low-resolution and electrospray ionization (ESI+) settings.

AFM Imaging

RADA16-I was prepared as described above. Once RADA16-I was purified the sample was made into a hydrogel by adding phosphate buffer solution at a concentration of 5 mg of peptide in 1 mL phosphate buffer solution. A 1 μL drop of this solution was taken out and diluted 50-fold by adding deionized water and mixed well. A 5 μL drop of the diluted sample

was added to freshly cleaved mica at room temperature for 1 min. The mica was then rinsed with Milli-Q water to remove the loosely bound fibrils before drying the mica with nitrogen gas.

The AFM image was collected in standard tapping mode (in the air) by a Dimension FastScan® Atomic Force Microscope (Bruker) under a dry nitrogen atmosphere using a single-beam silicon cantilever probe (Tap300AI-G (RESPA), resonance frequency is 320 kHz, normal force constant = 40 N/m). The data sets were subjected to first-order flattening using Nanoscope analysis software. The resolution was 512 x 512 pixels with a scanning speed of 0.5 Hz.

Solid-State NMR

Solid-state NMR experiments were performed on a Bruker 11.75 Tesla (500 MHz ^{1}H NMR frequency) spectrometer with a 2.5 mm magic angle spinning (MAS) probe. All reported chemical shifts were referenced to tetramethylsilane.

CPMAS[2] ^{1}H-^{13}C spectra were attained with 7-12 hours of signal averaging at 25 kHz MAS, with a constant 50 kHz radio frequency (rf) field applied to the ^{13}C channel during the ^{1}H-^{13}C CP spinlock (2 ms total contact time). Simultaneously during the CP spinlock, a linear ramp in ^{1}H pulse power was employed between 60 and 120 kHz rf field strength. A decoupling field of 110 kHz ^{1}H was applied using two pulse phase modulation (TPPM)[3] during successive acquisition of signal.

The 2D exchange fpRFDR experiments on Sample B were performed at 25 kHz MAS with 5 µs $\pi/2$ flip-back pulses for longitudinal mixing, 13.3 µs π pulses during fpRFDR recoupling, and 110 kHz TPPM ^{1}H decoupling.[4] The duration of fpRFDR recoupling was 1.28 ms (32 rotor periods).

Measurements of ^{13}C-^{13}C dipolar couplings were done using the PITHIRDS-CT pulse sequence[5] on selectively labeled samples (Samples C-F) at 12.5 kHz MAS and 16.7 μs π pulses during ^{13}C PITHIRDS dipolar recoupling. Recoupling was applied for a total of 61.44 ms, using $k_1 = 2, k_2 + k_3 = 32$, as defined by Tycko. Continuous wave ^{1}H decoupling at 110 kHz field strength was applied during the PITHIRDS-CT pulse sequence and 90 kHz continuous wave ^{1}H decoupling was applied during acquisition. Data analysis included natural abundance correction for the ^{13}C background as described previously.[6]

2D NMR ^{13}C-^{13}C exchange spectroscopy dipolar assisted rotational resonance (DARR) experiments for general long-range (< 0.6 nm) polarization transfers were performed on A4 C$_\beta$ sample (Figure S12).[7, 8] These experiments were performed with 10 kHz MAS and mixing times of 500 ms.

Circular Dichroism

The circular dichroism spectrum was collected at room temperature using a Jasco J-810 spectropolarimeter. RADA16-I nanofibers were prepared in 10 mM phosphate buffer using an identical procedure to that used to prepare solid-state NMR samples. Before the circular dichroism measurement, the nanofiber suspension was sonicated using a bath sonicator for 1 min. The spectrum was measured 15 min after sonication. The sample was measured inside a quartz cuvette with a path length of 0.01 mm.

Fourier Transform Infrared Spectroscopy

Fourier transform infrared spectroscopy was performed on RADA16-I nanofibers, as described previously, using a Thermo Scientific Nicolet 6700 spectrometer equipped with a TE cooled DTGS detector.[1] Lyophilized RADA16-I nanofibers were mixed with KBr and compressed to a

disk. ZnSe windows (0.55 mm) were positioned at a 35 ° tilt with respect to the infrared source in order to minimize interfringences.

Molecular Modeling of RADA16-I Nanofiber

The structural models of the RADA16-I nanofiber were built following the 8 possible classes of interfaces between β-sheets.[9] Only Classes 1, 3, and 5 were considered since only they have all the alanine sidechains exclusively buried in the interface. Model building started from a single β-strand generated by Ambertools 1.5. The strand was replicated and used to build a 20-strand parallel (for Classes 1 and 3) or antiparallel (for Class 5) β-sheet, using an inter-strand spacing of 0.49 nm.[10] The β-sheet was replicated and paired to produce the stacked β-sheets of the three classes, with interdigitated alanines. To describe the relative positioning between the β-sheets, we introduce a Cartesian coordinate system, with the x-axis defined as along one β-strand of one β-sheet, the y-axis within the β-sheet but perpendicular to the x-axis, and the z-axis perpendicular to the β-sheet. Relative to the first β-sheet, the second β-sheet was translated along the x direction for half of the spacing (0.65 nm) between two adjacent alanines in the same β-strand, along the y direction for half of the spacing between two adjacent β-strands in the same β-sheet, and along the z direction for ~0.6 nm to place the alanines from the two β-sheets to be roughly in the same plane perpendicular to the z-axis. Each model was then solvated in an $8 \times 12 \times 16$ nm^3 water box with NaCl at 0. 15 M, and energy minimized for 50,000 steps in NAMD 2.8.[11] The backbone □ and ψ angles in these models were around -123° and 123°, respectively.

The Class 3R2 model was built similarly to the Class 3 model, but the second β-sheet was not a replicate of the first β-sheet. Instead, the registry shifts of the two β-sheets occur in opposite directions. Arginine and aspartate sidechains were started at different rotameric states in multiple

molecular dynamics simulations. A larger water box, at $8 \times 14 \times 22$ nm^3, was used. After energy minimization, simulations at constant NPT were carried out, with periodic boundary condition imposed and a time-step of 1 fs. Van der Waals interactions were calculated with a switching distance of 1 nm and a cutoff of 1.2 nm, and updated every other step; electrostatic interactions were calculated by the particle mesh Ewald method[12] and updated every 4th step. For each simulation, the system was gradually heated to 300 K with a temperature increment of 50 K, for 100 ps at each temperature. After reaching 300 K, the simulations continued for 2 to 6 ns.

Simulations of PITHIRDS-CT NMR Experiments

Nuclear spin simulations were performed by running Spinevolution,[13] including the spins of 8 ^{13}C nuclei per simulation. For spin simulations in Figure 7, the atoms selected were the closest clusters of 8 ^{13}C atoms corresponding to specific ^{13}C-labeled sites within the molecular models, as illustrated in Figure S9. Simulated NMR parameters (*e.g.*, pulse powers, MAS speeds) matched those of the PITHIRDS-CT experiments. To reduce end effects related to missing ^{13}C-^{13}C couplings involving atoms not included in the simulations, initial simulated magnetization was on the most central atom only. The REPULSION scheme with 168 sets of Euler angles was employed for powder averaging.[14]

References

1. Cormier, A. R.; Ruiz-Orta, C.; Alamo, R. G.; Paravastu, A. K. Solid State Self-Assembly Mechanism of RADA16-I Designer Peptide. *Biomacromolecules* **2012**, 13, 1794-1804.

2. Schaefer, J.; Stejskal, E. C-13 Nuclear Magnetic-Resonance of Polymers Spinning at Magic Angle. *J. Am. Chem. Soc.* **1976**, 98, 1031-1032.

3. Bennett, A. E.; Rienstra, C. M.; Auger, M.; Lakshmi, K. V.; Griffin, R. G. Heteronuclear Decoupling in Rotating Solids. *J. Chem. Phys.* **1995**, 103, 6951-6958.

4. Ishii, Y. C-13-C-13 Dipolar Recoupling Under very Fast Magic Angle Spinning in Solid-State Nuclear Magnetic Resonance: Applications to Distance Measurements, Spectral Assignments, and High-Throughput Secondary-Structure Determination. *J. Chem. Phys.* **2001**, 114, 8473-8483.

5. Tycko, R. Symmetry-Based Constant-Time Homonuclear Dipolar Recoupling in Solid State NMR. *J. Chem. Phys.* **2007**, 126, 064506-064506.

6. Paravastu, A. K.; Leapman, R. D.; Yau, W. M.; Tycko, R. Molecular Structural Basis for Polymorphism in Alzheimer's Beta-Amyloid Fibrils. *P. Natl. Acad. Sci. USA* **2008**, 105, 18349-18354.

7. Morcombe, C. R.; Gaponenko, V.; Byrd, R. A.; Zilm, K. W. Diluting Abundant Spins by Isotope Edited Radio Frequency Field Assisted Diffusion. *J. Am. Chem. Soc.* **2004**, 126, 7196-7197.

8. Takegoshi, K.; Nakamura, S.; Terao, T. C-13-H-1 Dipolar-Assisted Rotational Resonance in Magic-Angle Spinning NMR. *Chem. Phys. Lett.* **2001**, 344, 631-637.

9. Sawaya, M. R.; Sambashivan, S.; Nelson, R.; Ivanova, M. I.; Sievers, S. A.; Apostol, M. I.; Thompson, M. J.; Balbirnie, M.; Wiltzius, J. J. W.; McFarlane, H. T., *et al.* Atomic Structures of Amyloid Cross-Beta Spines Reveal Varied Steric Zippers. *Nature* **2007**, 447, 453-457.

10. Nelson, R.; Sawaya, M.; Balbirnie, M.; Madsen, A.; Riekel, C.; Grothe, R.; Eisenberg, D. Structure of the Cross-Beta Spine of Amyloid-Like Fibrils. *Nature* **2005**, 435, 773-778.

11. Phillips, J.; Braun, R.; Wang, W.; Gumbart, J.; Tajkhorshid, E.; Villa, E.; Chipot, C.; Skeel, R.; Kale, L.; Schulten, K. Scalable Molecular Dynamics with NAMD. *J. Comput. Chem.* **2005**, 26, 1781-1802.

12. Darden, T.; York, D.; Pedersen, L. Particle Mesh Ewald - an N.Log(N) Method for Ewald Sums in Large Systems. *J. Chem. Phys.* **1993**, 98, 10089-10092.

13. Veshtort, M.; Griffin, R. G. SPINEVOLUTION: A Powerful Tool for the Simulation of Solid and Liquid State NMR Experiments. *J. Magn. Reson.* **2006**, 178, 248-282.

14. Bak, M.; Nielsen, N. C. REPULSION, a Novel Approach to Efficient Powder Averaging in Solid-State NMR. *J. Magn. Reson.* **1997**, 125, 132-139.

15. Bakota, E. L.; Sensoy, O.; Ozgur, B.; Sayar, M.; Hartgerink, J. D. Self-Assembling Multidomain Peptide Fibers with Aromatic Cores. *Biomacromolecules* **2013**, 14, 1370-1370-1378.

16. Cerf, E.; Sarroukh, R.; Tamamizu-Kato, S.; Breydo, L.; Derclaye, S.; Dufrene, Y. F.; Narayanaswami, V.; Goormaghtigh, E.; Ruysschaert, J. M.; Raussens, V. Antiparallel Beta-Sheet: A Signature Structure of the Oligomeric Amyloid Beta-Peptide. *Biochem J* **2009**, 421, 415-423.

17. Mukherjee, S.; Chowdhury, P.; Gai, F. Effect of Dehydration on the Aggregation Kinetics of Two Amyloid Peptides. *J Phys Chem B* **2009**, 113, 531-535.
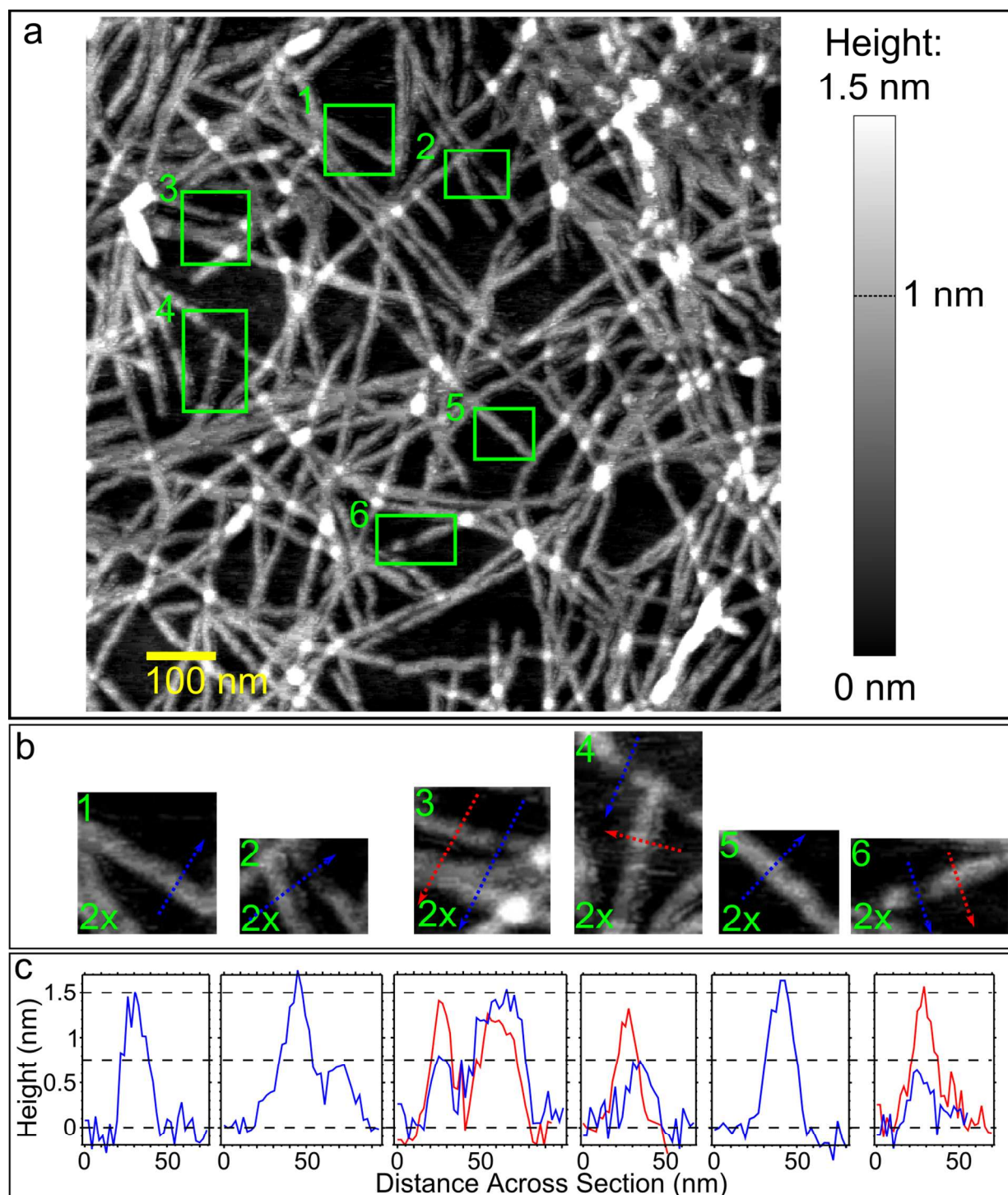
Figure S1. a) An AFM image of RADA16-I nanofibers after deposition onto mica and drying. b) Enlargements (2-fold) of regions indicated by green rectangles in (a). c) Sections from the AFM images indicated by blue and red dashed arrows in (b).

Table S1. NMR peak positions (δ) and line widths (lw) for RADA16-I signals from Sample B. Random coil values (RC) are also tabulated. All values are in ppm units, with estimated errors of ± 0.1 ppm for δ and lw.

	CO Chemical Shift			C_α Chemical Shift			C_β Chemical Shift		
	RC	δ	lw	RC	δ	lw	RC	δ	lw
R9	174.6	171.4	0.9	54.3	53.0	1.3	29.2	32.2	1.3
A10	176.1	173.0	1.3	50.8	49.2	1.4	17.4	20.8	0.7
					48.1	1.0		22.0	0.9
					48.6	1.4		23.4	0.8
D11	174.6	170.8	1.1	52.5	50.7	1.5	39.4	41.3	2.1

	C_γ Chemical Shift			C_δ Chemical Shift			C_ζ Chemical Shift		
	RC	δ	lw	RC	δ	lw	RC	δ	lw
R9	25.4	25.4	0.7	41.6	42.0	0.5	157.8	157.7	0.6
A10	-	-	-		-	-		-	-
D11	178.3	175.5	1.6		-	-		-	-
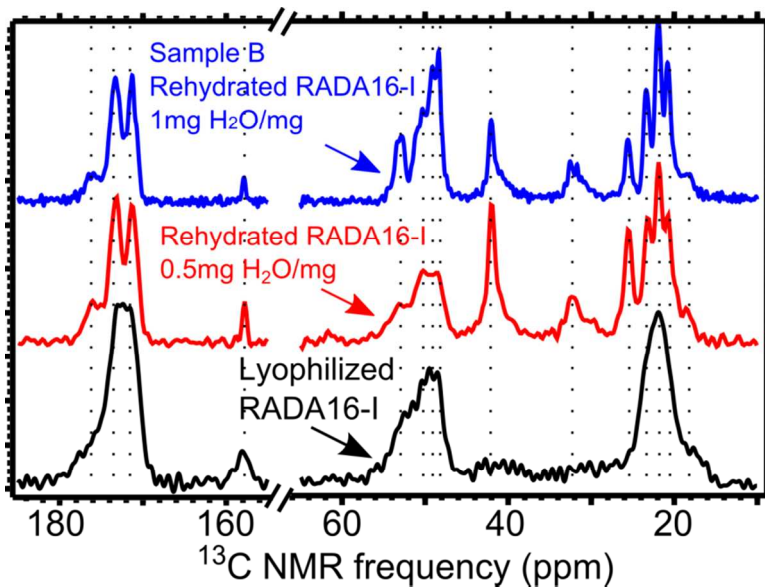
Figure S2. Natural abundance ^{1}H-^{13}C CPMAS NMR spectra of RADA16-I hydrogel lyophilized (black), rehydrated with 0.5 mg water/mg peptide (red), or 1 mg water/mg peptide (Sample B: blue).
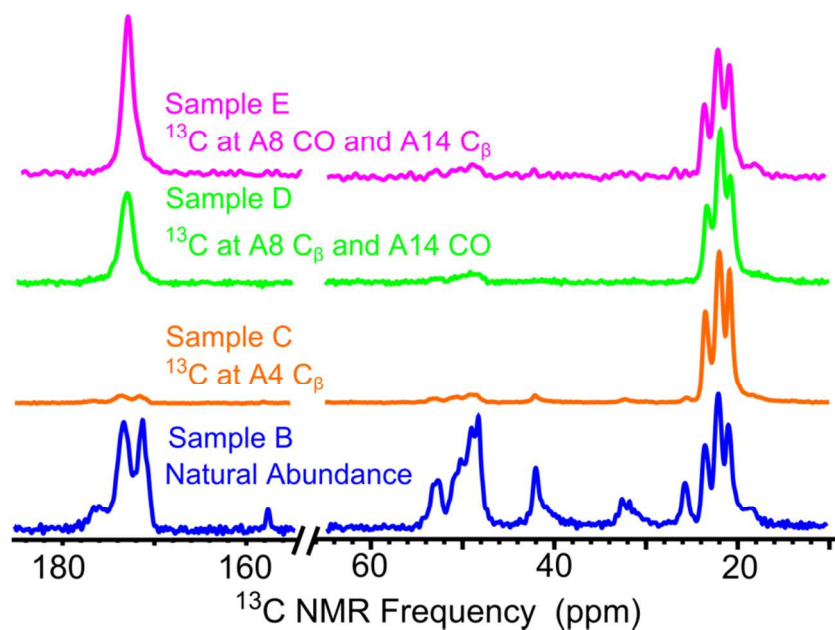
Figure S3. CPMAS NMR spectra for various labeled samples (Samples B, C, D, and E) showing methyl multiplicity.
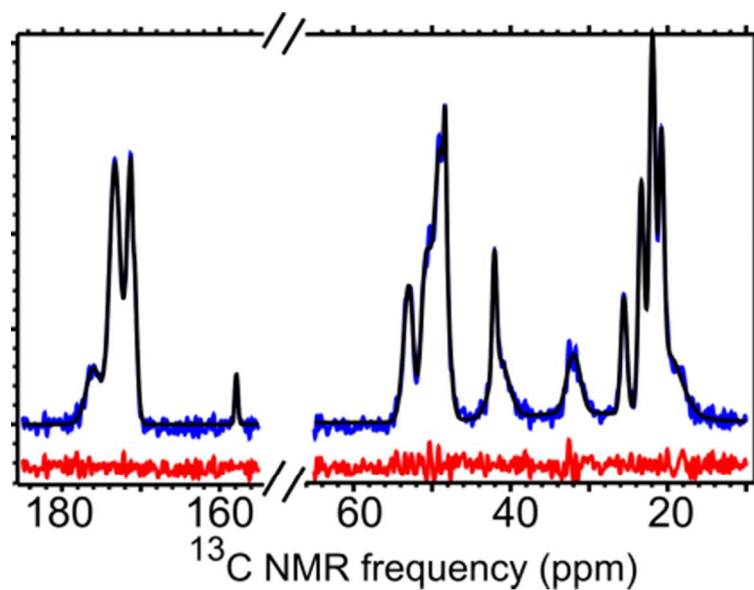
Figure S4. Nonlinear fit of the ^{1}H-^{13}C CPMAS spectrum of Sample B (blue) using a sum of Gaussian functions (best-fit curve in black). Residuals are shown in red.

Table S2. Peak positions (δ) for Sample B, deviation in peak position between Sample A and Sample B (Δ), and Sample B line widths (lw) in ppm. Unless otherwise specified, estimated error for δ and lw are ± 0.1 ppm and ± 0.1 ppm, respectively. Each amino acid is represented by a single letter abbreviation: A for alanine, R for arginine, and D for aspartate.

Amino Acid	CO Chemical Shift			C_α Chemical Shift			C_β Chemical Shift		
	δ	Δ	lw	Δ	Δ	lw	δ	Δ	lw
R	171.3	0.1	1.2	53	0	1.4	31.9	0.3	2.4
A	173.3	0.3	1.6	48.9	0.3	1.9	20.8	0	0.7
				48.2	-0.1	0.5	21.9	0.1	0.9
				48.2	0.4	0.5	23.4	0	0.9
							20.6±0.5*	-0.7	5.2
D	170.6	0.2	0.5	50.7	0	1.4	41.3	0	2.8

Amino Acid	C_γ Chemical Shift			C_δ Chemical Shift			C_ζ Chemical Shift		
	Δ	Δ	lw	Δ	Δ	lw	δ	Δ	lw
R	25.6	-0.2	0.9	42	0	0.7	158	-0.2	0.5
A	-	-	-	-		-	-		-
D	176	-0.5	2.1	-		-	-		-

*This peak position was assessed through line shape fitting of the CPMAS spectrum of Sample B, since crosspeaks to this signal were not observed in the 2D fpRFDR spectrum.
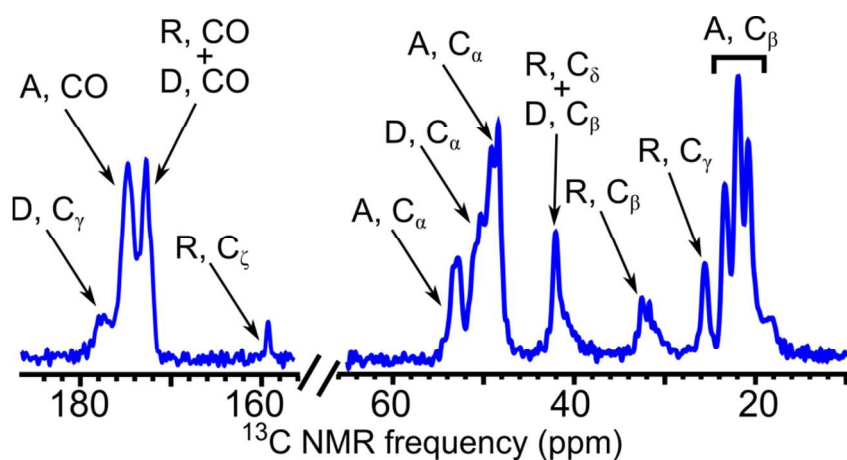
Figure S5. CPMAS NMR spectrum of Sample B, with assignments of chemical shifts. Each amino acid is represented by a single letter abbreviation: A for alanine, R for arginine, and D for aspartate.

Table S3. NMR peak positions for designated selectively ^{13}C-labeled RADA16-I samples with peak positions (δ) and line widths (lw) reported in ppm. Estimated error for both δ and lw values are ± 0.1 ppm.

Sample	Label	δ	lw	Sample	Label	δ	lw
C	A4 C_β	20.8	0.7	D	A14 CO	173.1	1.8
		21.9	0.9	E	A14 C_β	20.6	0.8
		23.5	0.8			21.9	1
D	A8 C_β	20.8	0.7			23.3	0.8
		22	0.9	E	A8 CO	173.5	1.6
		23.4	0.9				

Table S4. Estimates for   and ψ backbone torsion angles for each amino acid in the RADA16-I sequence based on the TALOS software and chemical shifts in Table S2. Since there are 3 peaks for each alanine C_β site; the TALOS calculation was repeated for each alanine C_β signal.

Residue	Position in Sequence	Alanine C_β Peak at 20.8 ϕ		ψ	
R	(-, 5, 9, 13)	-141	± 21	143	± 17
A	(6, 10, 14)	-135	± 20	142	± 17
D	(3, 7, 11, 15)	-138	± 21	139	± 15
A	(4, 8, 12, -)	-147	± 47	147	± 19

Residue	Position in Sequence	Alanine C_β Peak at 21.9 ϕ		ψ		Alanine C_β Peak at 23.4 ϕ		ψ	
R	(-, 5, 9, 13)	-124	± 18	131	± 14	-131	± 16	138	± 11
A	(2, 6, 10, 14)	-125	± 12	131	± 13	-131	± 12	141	± 16
D	(3, 7, 11, 15)	-118	± 21	134	± 17	-121	± 22	141	± 20
A	(4, 8, 12, -)	-128	± 18	140	± 17	-129	± 14	146	± 13
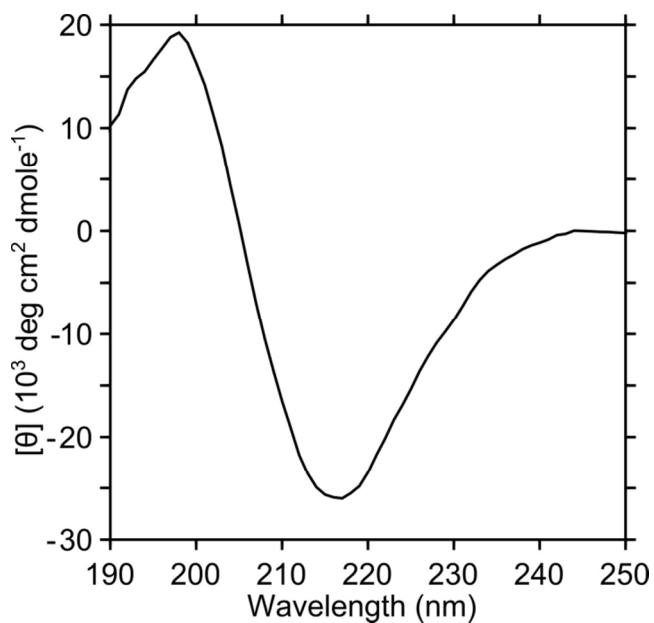
Figure S6. Circular dichroism spectrum for RADA16-I nanofibers.
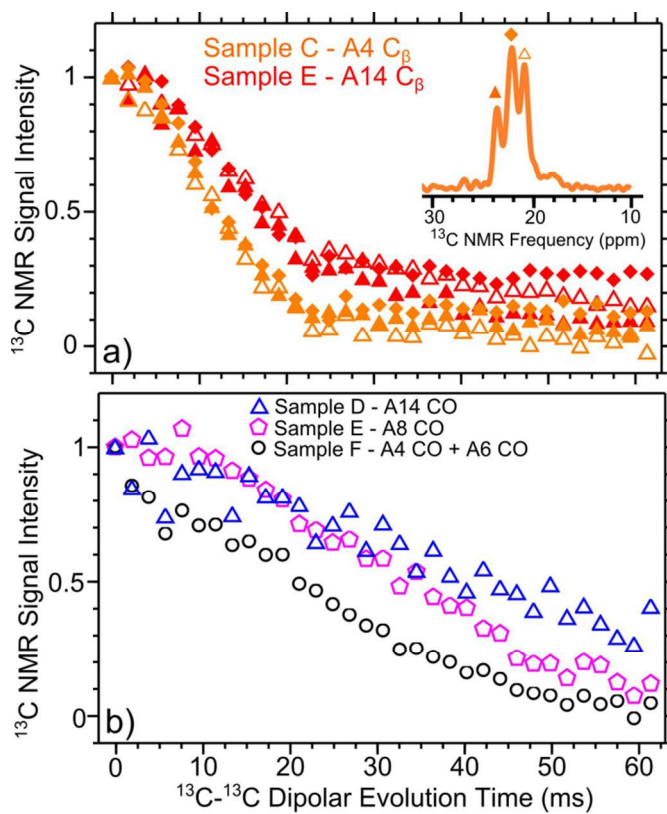
Figure S7. a) PITHIRDS-CT decays for A4 C_β (Sample C, orange) and A14 C_β (Sample E, red). b) PITHIRDS-CT decays for A14CO (Sample D, Blue), A8 CO (Sample E, magenta), and A4 and A6 CO (Sample F, black). Error bars are on the order of the symbol size.
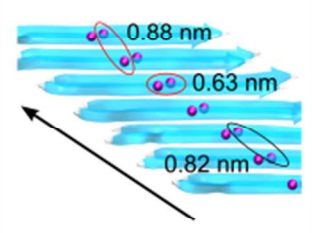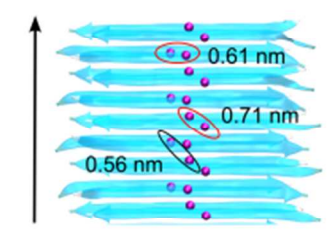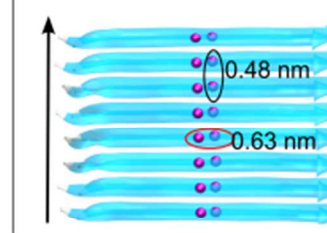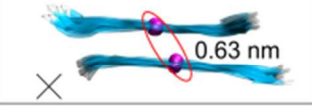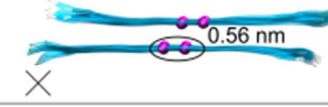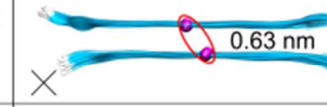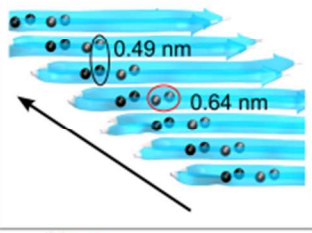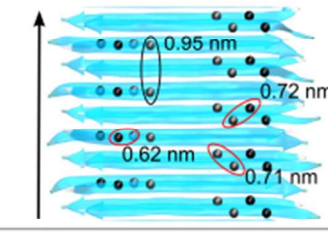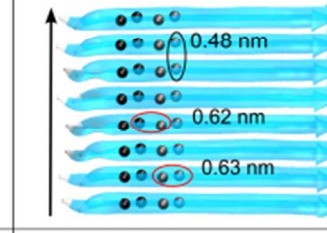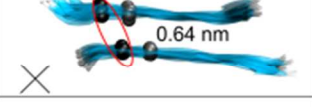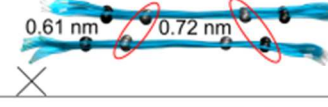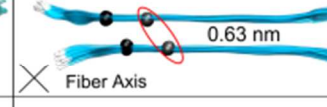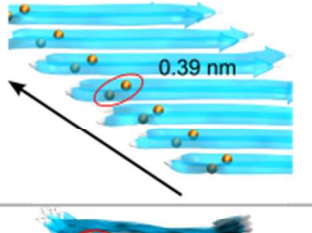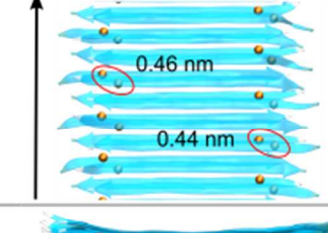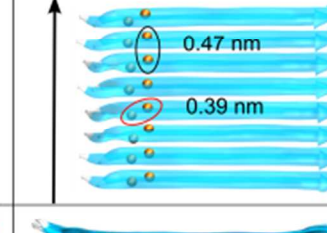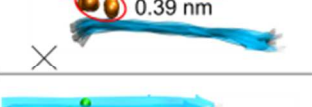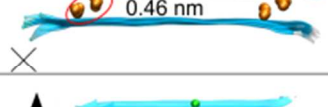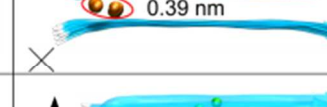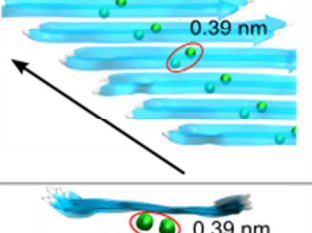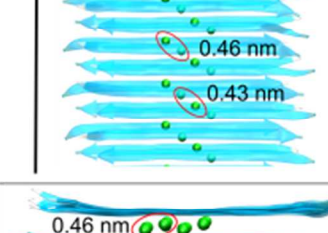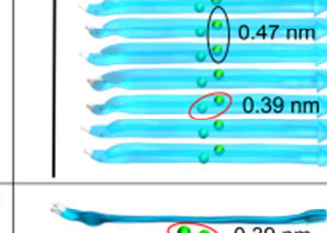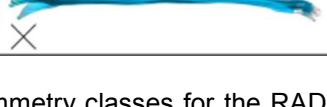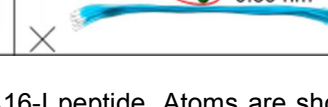
Figure S8. Molecular models of 3 symmetry classes for the RADA16-I peptide. Atoms are shown at CO and C_β positions of specified isotopic labels. For each panel, an arrow or x indicates the axis of the nanofiber. Inter-atomic distances are shown for pairs of atoms enclosed by ovals. Black or red ovals indicate atoms within the same β-sheet or between different β-sheets, respectively. The variation in distance from molecule to molecule between otherwise equivalent pairs of spins is approximately less than 8%.
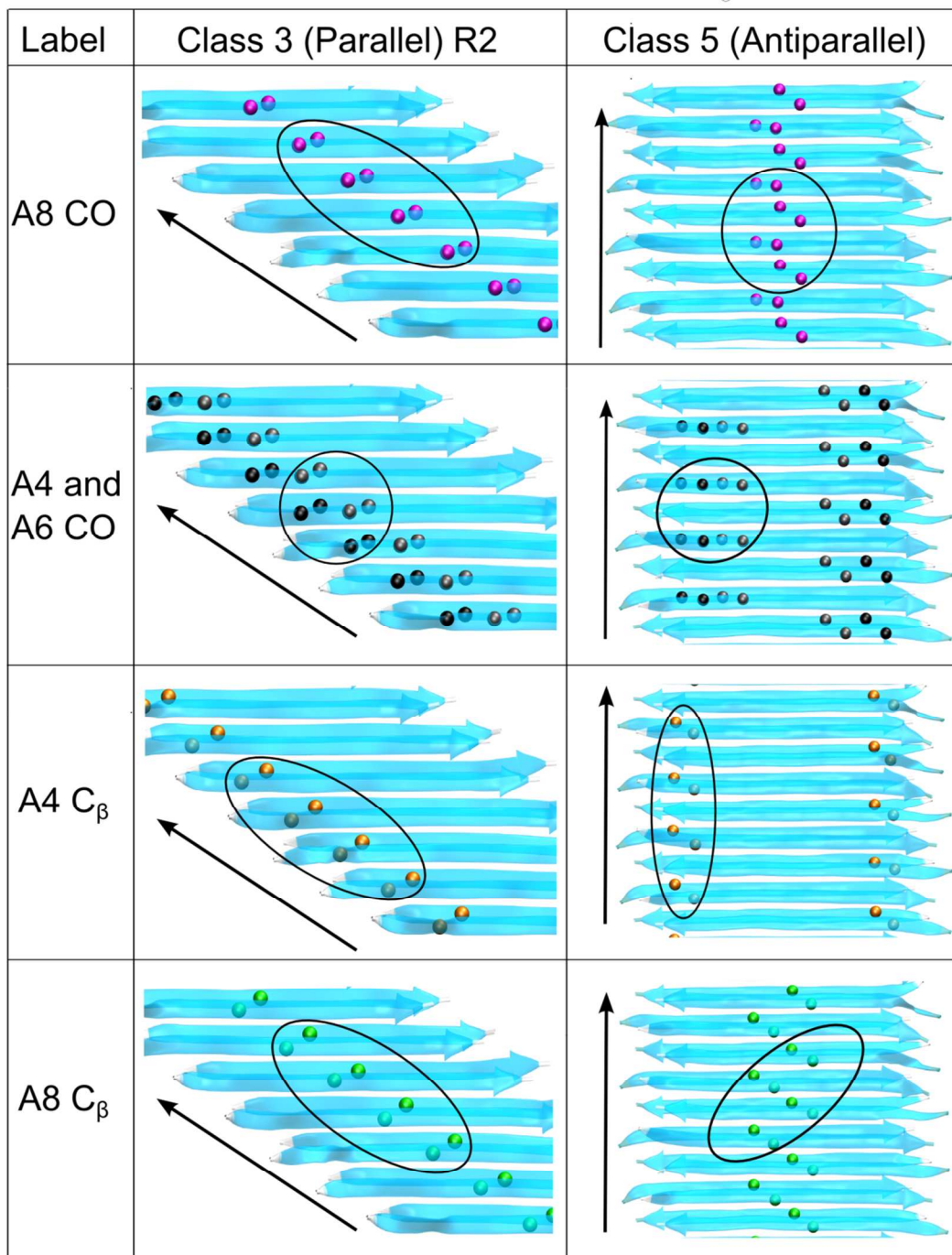
Figure S9. Positions of atoms used in PITHIRDS-CT spin simulations shown in Figure 7. Each simulation was limited to the 8 ^{13}C atoms, as indicated by the ovals.
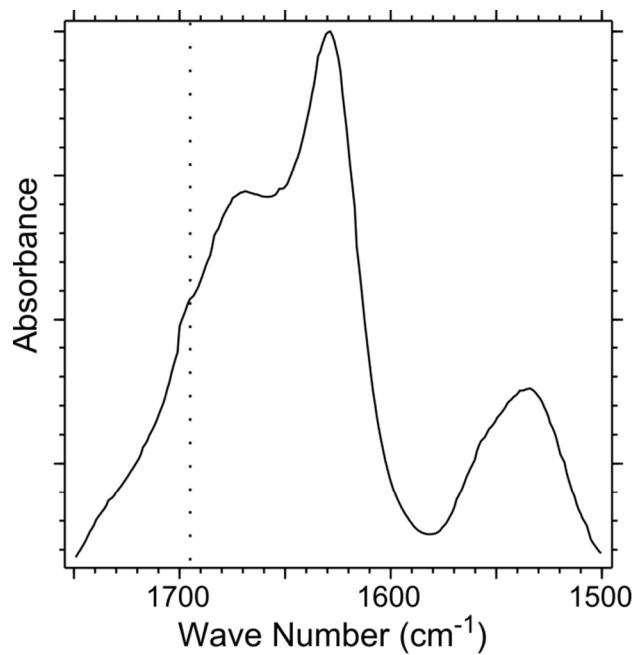
Figure S10. Amide I region of the Fourier transform infrared spectrum of lyophilized RADA16-I nanofibers. A vertical dotted line is shown at 1695 cm^{-1} to indicate that there is no resolved peak at this position, which has been shown to correlate to anti-parallel β-sheet structure.[15-17]

Table S5. Comparison of experimental structural constraints and RADA16-I nanofiber model predictions

| Structural Feature	Measured Value	Experimental Basis	Model Agreement		
			Class 3	Class 3R2	Class 5
Backbone torsion angles φ and ψ	See Table S4	TALOS predictions based on ^{13}C NMR chemical shifts obtained from 2D fpRFDR (Figure 2a) and CPMAS (Figure 2b)	Yes	Yes	Yes
^{13}C-^{13}C nuclear spacing for between A8 CO sites	0.6 nm	^{13}C PITHIRDS-CT (Figure 3b)	No	Yes	No
^{13}C-^{13}C nuclear spacing between A4 CO and A6 CO sites	0.5 nm	^{13}C PITHIRDS-CT (Figure 3)	No	Yes	No
Faster PITHIRDS-CT decay for A4 CO + A6 CO labeling compared to A8 CO labeling		^{13}C PITHIRDS-CT (Figure 3b)	No	Yes	No
^{13}C-^{13}C nuclear spacing between A4 C_β sites	0.4 nm	^{13}C PITHIRDS-CT (Figure 3b)	Yes	Yes	Yes
Identical PITHIRDS-CT decays for A4 Cβ and A8 Cβ		^{13}C PITHIRDS-CT (Figure S6a)	Yes	Yes	No
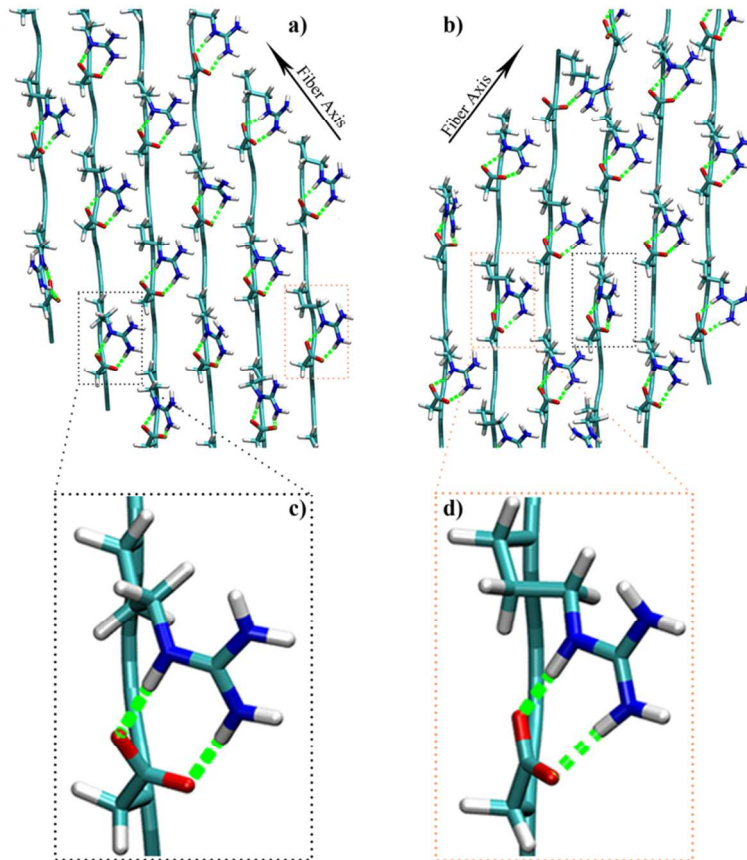
Figure S11. a) and b) Hydrogen-bonding patterns of arginine and aspartate sidechains formed on the outer faces of the two β-sheets in the Class 3R2 model. Within each β-strand, pairs of neighboring arginine and aspartate sidechains form similar hydrogen bonds in the two β-sheets. However, because the registry shifts in the two β-sheets occur in opposite directions, the hydrogen bonds are nearly perpendicular to the fiber axis in one β-sheet but parallel to the fiber axis in the other β-sheet. c) and d) Two different rotameric states of arginine that lead to the same bifurcated hydrogen bonds with a neighboring aspartate. The first three sidechain torsion angles of arginine in c) are all around 180°, but in d) the second torsion angle is changed to around 60°. Four arginine-aspartate pairs, with the arginines in either of the two rotameric states, are highlighted by a black or orange box in a) and b).
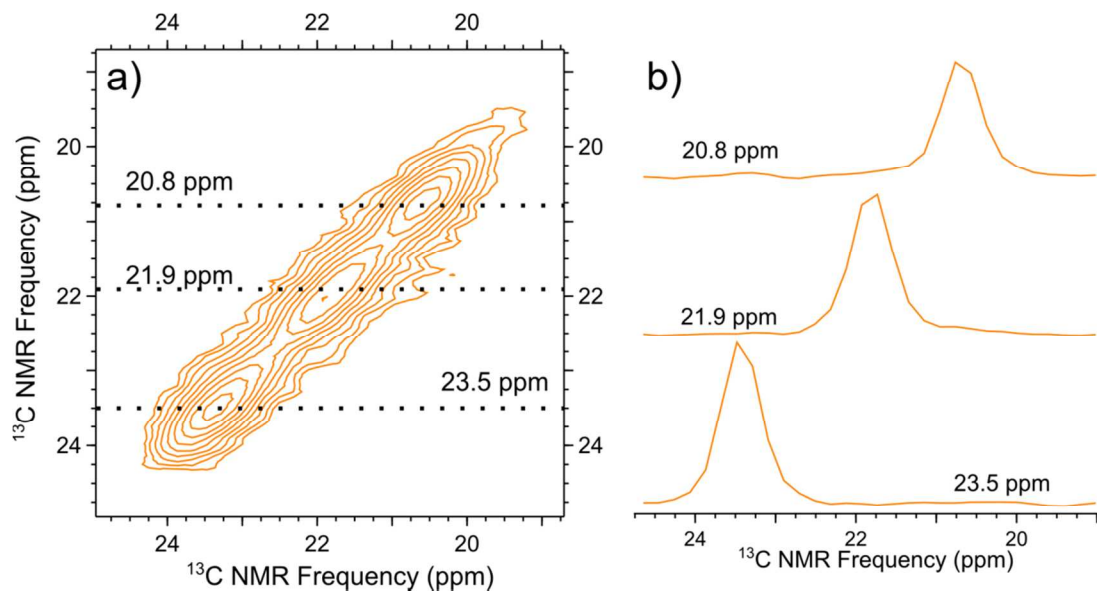
Figure S12. a) 2D-DARR spectrum of A4 C_β (Sample C) with dotted lines at positions of horizontal slices shown in (b).